




Statistical properties of structured random matrices

Eugene Bogomolny  and Olivier Giraud 
 Université Paris-Saclay, CNRS, LPTMS, 91405 Orsay, France

 (Received 6 January 2021; accepted 6 April 2021; published 20 April 2021)

Spectral properties of Hermitian Toeplitz, Hankel, and Toeplitz-plus-Hankel random matrices with independent identically distributed entries are investigated. Combining numerical and analytic arguments it is demonstrated that spectral statistics of all these low-complexity random matrices is of the intermediate type, characterized by: (i) level repulsion at short distances, (ii) an exponential decrease in the nearest-neighbor distributions at long distances, (iii) a nontrivial value of the spectral compressibility, and (iv) the existence of nontrivial fractal dimensions of eigenvectors in Fourier space. Our findings show that intermediate-type statistics is more ubiquitous and universal than was considered so far and open a new direction in random matrix theory.

DOI: [10.1103/PhysRevE.103.042213](https://doi.org/10.1103/PhysRevE.103.042213)

I. INTRODUCTION

Matrices are omnipresent structures in extremely varied branches of physics and mathematics, and there exist many different types of matrices tailored for specific problems. To get a certain overview of a general matrix classification one could order matrices according to their complexity. The well-known Kolmogorov complexity of a string is the minimal length of a program which can calculate the string. A possible way to measure the (arithmetic) complexity of a matrix is by counting the minimal number of operations needed to perform certain nontrivial operations, e.g., to find the inverse matrix, or matrix eigenvalues, with a given precision (see, e.g., Refs. [1–4] and references therein).

For generic $N \times N$ matrices, standard algorithms (such as the Gauss-Jordan elimination) require $O(N^3)$ operations, although more refined algorithms reduce it (up to logarithmic corrections) to $O(N^3)$ with $\omega \approx 2.37286$ [4]. Nevertheless, there exist special types of matrices of lower complexity which generically necessitate a smaller number of operations.

The most investigated class of such low-complexity matrices consists of matrices with small-rank displacement structure [5,6] which are characterized by the existence of a linear operator that transforms all matrices from the class into matrices of small rank. Two main types of such displacement operators were used, the Toeplitz-like displacement operator $\nabla_{A,B}(M) = M - AMB$ and the Hankel-like displacement operator $\Delta_{A,B}(M) = AM - MB$, where A and B are arbitrary matrices. The rank of matrices $\nabla_{A,B}(M)$ and $\Delta_{A,B}(M)$ depends on the choice of A and B ; the minimal rank r is called the displacement rank of M . A matrix is referred to as a structured matrix if its displacement rank is much smaller than its dimension. The importance of this notion comes from the theorem proved in Ref. [5] that the standard $O(N^3)$ number of operations needed, e.g., to inverse a matrix can be replaced by $O(rN^2)$. By using more sophisticated algorithms, this number can even be reduced to $O(rN \ln N)$ [7–9].

The best-known examples of structured matrices are Toeplitz (T_{mn}), Hankel (H_{mn}), and Toeplitz-plus-Hankel $[(T + H)_{mn}]$ matrices, whose matrix elements have the following form

$$T_{mn} = t_{m-n}, \quad H_{mn} = h_{m+n}, \quad (T + H)_{mn} = t_{m-n} + h_{m+n}, \quad (1)$$

with $m, n = 1, \dots, N$ and t_i, h_j arbitrary real or complex numbers. The matrices considered in (1) have a long history: Hankel matrices were introduced in 1861 [10] and Toeplitz matrices in 1911 [11]. They appear naturally in various fields of mathematics and physics, such as differential and integral equations, functional analysis, probability theory, statistics, numerical analysis, theory of stationary processes, signal and image processing, control theory, integrable models, among many others (see, e.g., Refs. [12–18] and references therein). The existence of algorithms inverting these matrices in $O(N^2)$ operations were known for a long time [8,19–22]. Examples of displacement structures for these matrices is briefly discussed in Appendix A. Considerable efforts were performed to find the asymptotic behavior of the determinants and eigenproblems for matrices (1) in the limit of large matrix dimensions (see, e.g., Refs. [16–18] and references therein). It appeared that all these calculations require additional regularity conditions of matrix elements (e.g., a finite number of Fisher-Hartwig singularities). Very irregular matrices, that is, without any particular structure other than (1), seem to be inaccessible to known analytic methods.

The investigation of irregular Hermitian Toeplitz matrices was initiated in Ref. [23] where elements t_k were taken as independent and identically distributed (i.i.d.) random variables (with $t_{-k} = t_k^*$). A central aspect of the study of random matrices is the investigation of their statistical spectral properties. From the above-mentioned fact that Toeplitz matrices are low-complexity matrices it seems natural that their spectral statistics differ from the Wigner-Dyson statistics of usual random matrix ensembles used to describe chaotic systems [24].

It was shown in Ref. [23] that spectral statistics of random Toeplitz matrices is of intermediate type, which is characterized by level repulsion, as for usual random matrix ensembles [25] but with exponential decrease in nearest-neighbor spacing distributions as for the Poisson distribution typical for integrable models [26]. Such a type of intermediate spectral statistics was first observed in the Anderson model at the point of metal-insulator transition [27,28] and later in certain pseudointegrable billiards [29,30] and quantum maps [31]. More precisely, Ref. [23] showed that spectral statistics of random Toeplitz matrices are well described by the semi-Poisson distribution, which is the simplest model where only the nearest-neighbor levels interact (an approach described in Ref. [32]).

The main purpose of this paper is to investigate statistical properties of other structured matrices beyond the Toeplitz class, namely, random Hermitian Hankel and Toeplitz-plus-Hankel matrices where elements t_k and h_k in (1) are i.i.d. Gaussian random variables with zero mean and unit variance (for complex elements real and imaginary parts are i.i.d. standard Gaussian random variables). The main conclusion of the paper is that spectral statistics of all these low-complexity matrices is of intermediate type and well described by a γ distribution. Moreover, eigenvectors of these matrices are multifractal in Fourier space, which is typical for models with intermediate statistics. Such a multifractal behavior of eigenstates was identified in wave functions of the Anderson model at metal-insulator transition [33–35] and in certain random matrix ensembles [36]. Quite remarkably, as we show here, such features are also present in models as simple as random Toeplitz or Hankel matrix ensembles.

The plan of the paper is the following. Section II is devoted to the investigation of a simple heuristic method which permits to obtain explicit approximate formulas for spectral statistics of structured matrices. These results are then applied to random Hermitian Toeplitz, Hankel, and Toeplitz-plus-Hankel matrices with independent matrix elements. The results demonstrate the intermediate character of spectral statistics for these matrices and confirm the fact, observed in Ref. [23], that random Toeplitz matrices are well approximated by the semi-Poisson distribution. Other functions characterizing the spectrum are discussed in Sec. III. In Sec. IV it is demonstrated that the results of direct large-scale numerical calculations for different correlation functions for the above matrices agree well with the obtained approximate formulas. The summary of the obtained results is performed in Sec. V. In Appendix A the simplest displacement structures for the considered matrices are briefly discussed. Appendix B is devoted to the construction of short-range plasma models which have the same power-low behavior at small arguments as matrices discussed in the main text.

II. WIGNER-TYPE APPROXIMATE FORMULAS

The purpose of the present section is to obtain heuristically simple approximate formulas for structured random matrices. Our guiding principle is the construction of the Wigner-type surmises for nearest-neighbor distributions in standard Wigner-Dyson ensembles of random matrices.

A. Wigner-Dyson ensembles

The usual Wigner-Dyson ensembles of random matrices are the Gaussian orthogonal ensemble, the Gaussian unitary ensemble, and the Gaussian symplectic ensemble characterized, respectively, by the Dyson index $\beta = 1, 2, 4$. For these ensembles, it is well known (see, e.g., Refs. [25,37]) that the nearest-neighbor spacing distribution $P_0(s)$ (i.e., the probability that two levels are separated by a distance s with no level inbetween) is well approximated by the Wigner surmise,

$$P_0(s) = a(\beta)s^\beta e^{-b(\beta)s^2}, \quad (2)$$

with constants $a(\beta)$ and $b(\beta)$ determined from the normalization conditions,

$$\int_0^\infty P_0(s)ds = 1, \quad \int_0^\infty sP_0(s)ds = 1. \quad (3)$$

The success of such a surmise is based on the simple fact that any function which has the correct behavior $\sim s^\beta$ at small values of the argument and is quickly decreasing at large values of the argument should be a reasonably good approximation for the true function, provided normalization fixes the otherwise arbitrary parameters $a(\beta)$ and $b(\beta)$. Of course, deviations between the exact result and the simple expression (2) do exist, but as the function at large argument is small, they are practically unobserved. The accuracy of the Wigner surmise is so high that the exact function, given by a solution of a certain Painlevé equation [25,38], is very rarely used, mainly in monumental calculations of the Riemann ζ function [39]. In most other cases the Wigner surmise is sufficient.

Much less used are the analogous Wigner-type surmises for the higher-order nearest-neighbor spacing distributions $P_n(s)$, which are the probabilities that two eigenvalues are separated by a distance s with exactly n eigenvalues between them. Again, the accuracy of such an approximate formula for $P_n(s)$ mainly depends on the correctness of the small- s behavior and of the quick asymptotic decrease in the function at large argument. The main ingredient to obtain these surmises is, therefore, to determine the small-argument behavior of $P_n(s)$. This can be readily obtained from the exact joint eigenvalue probability density, which for the Wigner-Dyson random matrix ensembles is known to be [25]

$$P(e_1, \dots, e_N) \sim \prod_{1 \leq i < j \leq N} |e_i - e_j|^\beta \prod_{k=1}^N e^{-V(e_k)}, \quad (4)$$

where $V(e)$ is a confining potential and $\beta = 1, 2, 4$. The matrices that contribute most to $P_n(s)$ for $s \sim 0$ are those for which $n+2$ eigenvalues are close to a certain value λ and, thus, almost degenerate with a distance $s \ll 1$ between the largest and the smallest of these eigenvalues (see Fig. 1). If we assume that all other eigenvalues are separated from λ by a gap $\gg s$, then the product $\prod_{i < j}$ over all pairs of eigenvalues in (4) splits into two parts: A first product Π_1 involving only those eigenvalues that are close to λ , and a second product Π_2 including all the other terms. In product Π_2 , eigenvalues close to λ are paired with eigenvalues far from λ and, thus, can be replaced by λ . Under this approximation, only product Π_1 will contribute to the small- s behavior of $P_n(s)$. This product Π_1 can be expressed solely in terms of spacings s_1, \dots, s_{n+1}

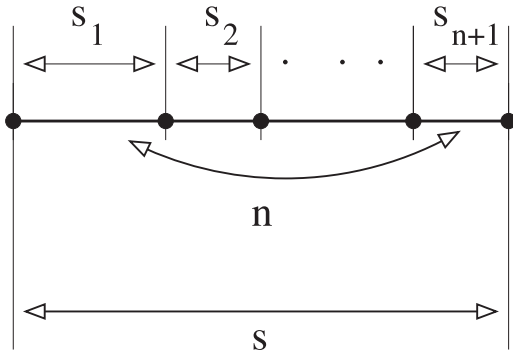


FIG. 1. Configuration of eigenvalues for the $P_n(s)$ correlation function.

between consecutive eigenvalues close to λ (see Fig. 1). At small s the confining potential can be discarded, and we, thus, have

$$P_n(s) \underset{s \rightarrow 0}{\sim} \int_0^\infty ds_1 ds_2 \cdots ds_{n+1} \prod_{k=0}^n \prod_{i=1}^{n-k+1} (s_i + \cdots + s_{i+k})^\beta \delta\left(s - \sum_{k=1}^{n+1} s_k\right). \tag{5}$$

Substituting $s_k = sy_k$ in (5) one can extract the leading power of s by merely counting the different contributions (the δ function accounting for a -1 contribution); the remaining integral just gives an overall multiplicative constant. One directly gets

$$P_n(s) \underset{s \rightarrow 0}{\sim} s^{\gamma_n}, \quad \gamma_n = \beta \frac{(n+2)(n+1)}{2} + n. \tag{6}$$

Assuming, as in the usual Wigner surmise, that all correlation functions have Gaussian decay at a large argument one gets an approximate formula for $P_n(s)$ of the form

$$P_n(s) = a_n s^{\gamma_n} \exp(-b_n s^2), \tag{7}$$

where constants a_n and b_n are calculated from the standard normalization conditions,

$$\int_0^\infty P_n(s) ds = 1, \quad \int_0^\infty s P_n(s) ds = n + 1. \tag{8}$$

These formulas are not new and have been derived in, e.g., Ref. [40] and (from different considerations) in Ref. [41].

The main drawback of the above approach is that it requires the knowledge of the exact eigenvalue distribution. Now we will obtain the same result from simple arguments, without using the specific form (4) and extend it to more general situations.

B. Wigner-Dyson revisited and intermediate-type statistics

Suppose, as above, that the small- s behavior of $P_n(s)$ comes from matrices with $n + 2$ eigenvalues close to a certain fixed value λ and all other eigenvalues far away from λ (here and in the following we restrict ourselves to the vicinity of the bulk of the spectrum, that is, $\lambda \simeq 0$ for Wigner-Dyson matrices). This means that only eigenvalues close to λ contribute to $P_n(s)$ as $s \rightarrow 0$, and the other eigenvalues can be ignored. One can

then restrict oneself to a $(n + 2) \times (n + 2)$ Hermitian matrix M_{ij} whose eigenvalues are almost degenerate, that is

$$M_{ij} = \lambda \delta_{ij} + \epsilon m_{ij}, \quad |\epsilon| \ll 1. \tag{9}$$

We are looking for the number of independent variables in m whose nonzero values lift the degeneracy. Since that matrix is Hermitian, the total number of independent matrix elements is $N_t = n + 2 + \beta \binom{n+2}{2}$ with $\beta = 1$ for real and $\beta = 2$ for complex matrices. But adding a constant value to all m_{ij} does not change the relative position of eigenvalues so that this number has to be diminished by 1 (one could, e.g., impose that $m_{11} = 0$). Therefore, we get

$$q_n = n + 1 + \beta \binom{n + 2}{2} \tag{10}$$

variables whose nonzero values lift the degeneracy.

Let e_j be eigenvalues of M_{ij} . Setting $e_j = \lambda + \epsilon v_j$ for $j = 1, \dots, n + 2$, the v_j are solutions of $\det(v \delta_{ij} - m_{ij}) = 0$. When $m_{ij} = O(1)$ all e_j are, in general, different and are of the order of ϵ around λ . For the considered ensembles all q_n matrix elements are independent random variables with a certain nonzero probability density. The spacing distribution is then obtained by a q_n -fold integral over these variables. The probability that all eigenvalues of matrix M_{ij} are within a short distance s from λ is the probability of the event that all the q_n variables are on the order of s . One can, therefore, rescale each variable in the q_n -fold integral by s , which gives a probability proportional to s^{q_n} , and, thus,

$$P(|e_j - \lambda| < s) \underset{s \rightarrow 0}{\sim} s^{q_n}. \tag{11}$$

This quantity corresponds to the cumulative spacing distribution $\int_0^s P_n(y) dy$. Therefore, the spacing distribution $P_n(s)$ has the following limiting value:

$$P_n(s) \underset{s \rightarrow 0}{\sim} s^{\gamma_n}, \quad \gamma_n = q_n - 1. \tag{12}$$

For the Wigner-Dyson ensembles q_n is given by (10), thus, this expression agrees with the above result (6) obtained from the exact joint distribution. The behavior of $P_n(s)$ at large values of the argument is then determined by the fact that each eigenvalue interacts with all other eigenvalues, which suggests the quadratic exponent in (7).

The number q_n is known as the codimension of the matrix ensemble. More precisely, for a family of matrices $M(x)$ that depend on a parameter $x \in \mathbb{R}^m$, one can define the submanifold of parameter space $\mathcal{M} \subset \mathbb{R}^m$ such that for all $x \in \mathcal{M}$ the matrix $M(x)$ has k degenerate eigenvalues equal to λ . The dimension $\dim(\mathcal{M})$ gives the number of variables that can be modified without changing the k eigenvalues λ . Then the codimension of the matrix ensemble is defined as the codimension of the submanifold \mathcal{M} ; it determines the minimal number of independent parameters in a matrix that has k degenerate eigenvalues with a given value.

In the present case, q_n gives the minimal number of independent parameters in a Hermitian matrix with $n + 2$ degenerate eigenvalues. The well-known theorem of von Neumann and Wigner [42] (see also [43]) states that the codimension of Hermitian matrices with k degenerate eigenvalues is $k^2 - 1$ for complex matrices and $\frac{1}{2}(k + 2)(k - 1)$ for real

ones. When $k = n + 2$ these expressions agree with q_n in Eq. (10) obtained from matrices of size $n + 2$.

We are unaware of exact results about codimensions for matrix families considered in the paper. Nevertheless, the codimensions of any subclass of Hermitian matrices are independent of matrix dimensions as they are upper bounded by the above size-independent values. It is then natural to conjecture that they can be determined by considering the smallest possible matrix with $n + 2$ degenerate eigenvalues. The above discussion shows that such an approach works well for the Wigner-Dyson ensembles. Below it will be applied to Hermitian Toeplitz, Hankel, and Toeplitz-plus-Hankel ensembles of random matrices.

In order to get a complete Wigner-like surmise we must additionally fix the behavior at large argument. In the case of the intermediate-type ensembles considered in the present paper one can argue [27–29] that the interaction between eigenvalues has to be of short range and asymptotically the nearest-neighbor distributions decrease only as an exponential of the distance between eigenvalues (which is typical in short-range interaction thermodynamics). Combining both asymptotic behaviors at large and small s , one gets that the Wigner-like surmise for intermediate-type matrices should be of the form

$$P_n(s) = a_n s^{\gamma_n} \exp(-b_n s), \tag{13}$$

where a_n and b_n are fixed by the normalization conditions (8), that is,

$$a_n = \frac{1}{\Gamma(\gamma_n + 1)} \left(\frac{\gamma_n + 1}{n + 1} \right)^{\gamma_n + 1}, \quad b_n = \frac{\gamma_n + 1}{n + 1}. \tag{14}$$

The distribution (13) belongs to the family of γ distributions. It is determined by the quantity $\gamma_n = q_n - 1$ only with q_n being the minimal number of independent matrix elements in a small vicinity of a degenerate matrix such that any variations of them lift the degeneracies of matrix eigenvalues. Another definition of q_n is that it is equal to the total number of parameters minus the number of “zero modes”, that is, the number of parameters whose variation does not remove the eigenvalue degeneracy.

C. Toeplitz matrices

Let us now consider a random $(n + 2) \times (n + 2)$ Hermitian Toeplitz matrix $T_{jk} = t_{j-k}$, $1 \leq j, k \leq n + 2$, where t_i ’s are real or complex i.i.d. Gaussian random variables. A Hermitian Toeplitz matrix of size $n + 2$ has $n + 1$ distinct off-diagonal elements and a single real diagonal entry. In total this gives $N_t = 1 + \beta(n + 1)$ independent variables, where $\beta = 1$ for real and $\beta = 2$ for complex matrices.

If a degenerate matrix is perturbed by a Toeplitz matrix \mathfrak{T} in such a way that the perturbation does not lift the degeneracy, then \mathfrak{T} has to be proportional to the identity matrix, $\mathfrak{T} = \lambda \mathbb{1}$. There is only one such matrix with $t_0 = \lambda$ and all other elements zero. It implies that there exists only one zero mode. Therefore, $q_n = N_t - 1 = \beta(n + 1)$ and, consequently,

$$\gamma_n = \beta(n + 1) - 1. \tag{15}$$

The γ distribution (13) with such γ_n and $\beta = 1$ corresponds to the Poisson distribution, whereas for $\beta = 2$ it coincides with

the semi-Poisson distribution, which agrees with the results of Ref. [23] for random Toeplitz matrices.

D. Special Toeplitz-plus-Hankel matrices

We now apply the same method to Hermitian Toeplitz-plus-Hankel matrices having the form $t_{i-j} + h_{i+j}$. Elements h_i may either be independent from the elements t_j or depend on them. Let us start with the second situation, where entries of the Hankel matrix are given in terms of the t_j . This situation arises when considering the spectrum of a real symmetric Toeplitz matrix. Indeed, it is well known that the spectrum of such a matrix can be split into two sets of eigenvalues, the so-called reciprocal and antireciprocal sets, associated with symmetric and skew-symmetric eigenvectors, respectively [44,45]. These sets (for real Toeplitz matrices of even dimension) are given by eigenvalues of matrices of the form

$$(T + \eta H)_{ij} = t_{|i-j|} + \eta t_{i+j-1}, \tag{16}$$

where $\eta = \pm 1$ and t_i are real i.i.d. Gaussian random variables.

Any $(n + 2) \times (n + 2)$ matrix of the form (16) is determined by the $N_t = 2n + 4$ elements t_0, \dots, t_{2n+3} . Once again, the identity matrix belongs to this ensemble, thus, the number of zero modes corresponds to the number of parameters for which a matrix (16) is proportional to the identity,

$$\mathfrak{T} + \eta \mathfrak{H} = \lambda \mathbb{1}. \tag{17}$$

Such a matrix has only two free parameters. Indeed, it is subjected to the restrictions $t_{ij} + \eta h_{ij} = \lambda \delta_{ij}$, yielding for $t_{ij} = t_{|i-j|}$ and $h_{ij} = t_{i+j-1}$,

$$t_0 + \eta t_{2i-1} = \lambda, \quad i = 1, \dots, n + 2, \tag{18}$$

$$t_{i-j} + \eta t_{i+j-1} = 0, \quad i = j + 1, \dots, n + 2. \tag{19}$$

Condition (18) is equivalent to

$$\eta t_{2i-1} = \lambda - t_0, \quad i = 1, \dots, n + 2, \tag{20}$$

which fixes all odd coefficients in terms of λ and t_0 , whereas condition (19) taken at $i = j + 1$ gives

$$t_{2j} = -\eta t_1, \quad j = 1, \dots, n + 1, \tag{21}$$

which fixes all even coefficients apart from t_0 . The two remaining free parameters are, thus, t_0 and λ , yielding two zero modes. The number of independent parameters minus the number of zero modes is then $q_n = N_t - 2 = 2n + 2$, and one gets for these matrices,

$$\gamma_n = 2n + 1, \tag{22}$$

which corresponds to the semi-Poisson distribution. Again, this is in agreement with the findings in Ref. [23].

E. Independent Toeplitz-plus-Hankel matrices

Suppose now that coefficients of the Toeplitz and Hankel matrices are fully independent. Namely, we consider Toeplitz-plus-Hankel matrices of the form

$$(T + H)_{ij} = t_{i-j} + h_{i+j}, \quad i, j = 1, \dots, n + 2, \tag{23}$$

with independent (real or complex) coefficients t_j , $j = 0, 1, \dots, n + 1$ and real h_j , $j = 2, \dots, 2n + 4$. The total number of parameters is now $N_t = 1 + \beta(n + 1) + (2n + 3)$.

As in the previous subsections to find zero modes one has calculate the number of matrices from this ensemble such

$$\mathfrak{T} + \mathfrak{H} = \lambda \mathbb{1}. \tag{24}$$

This condition now yields the restrictions

$$t_0 + h_{2i} = \lambda, \quad i = 1, \dots, n + 2, \tag{25}$$

$$t_{i-j} + h_{i+j} = 0, \quad i = j + 1, \dots, n + 2. \tag{26}$$

The first condition entails that $h_{2i} = \lambda - t_0$ for $i = 1, \dots, n + 2$, whereas the second condition for $1 \leq j \leq n + 1$ and $i = j + k$ gives

$$h_{2j+k} = -t_k, \quad k = 1, \dots, n + 2 - j. \tag{27}$$

In particular, $h_{2j+1} = -t_1$ for $1 \leq j \leq n + 1$, and, thus, all h_j 's are fixed. Equation (27) fixes, in turn, all t_k 's for $k \geq 2$, and constrains the imaginary part of t_1 to be zero. Only t_0 , λ , and the real part of t_1 remain free, providing three zero modes. Therefore, one has $q_n = N_t - 3 = 2n + 1 + \beta(n + 1)$. It means that for independent Toeplitz-plus-Hankel matrices $\gamma_n = 2n + \beta(n + 1)$. This gives

$$\gamma_n = 3n + 1 \quad \text{for } \beta = 1, \tag{28}$$

$$\gamma_n = 4n + 2 \quad \text{for } \beta = 2. \tag{29}$$

F. Hankel matrices

Let us now turn to an ensemble of pure Hankel matrices H_{jk} with entries of the form h_{i+j} . Whereas in all cases considered so far the identity matrix was a member of the ensemble, this is not the case anymore: A Hankel matrix cannot have all eigenvalues equal since the identity matrix is not of Hankel form (this also reflects in the peculiar density of eigenvalues for this ensemble as compared with the others as will be illustrated in Fig. 2 below). Spectra with $n + 2$ almost degenerate eigenvalues can nevertheless be obtained by considering matrices of size $N = 2n + 2$. Indeed, the $N \times N$ Hankel matrix,

$$d_{jk}(N) = \begin{cases} 1, & j + k \equiv 0 \pmod{N}, \\ 0, & j + k \not\equiv 0 \pmod{N}, \end{cases} \tag{30}$$

with $N = 2n + 2$ has $n + 2$ eigenvalues equal to 1 and n eigenvalues -1 , therefore, in the vicinity of $d(N)$ matrices have $n + 2$ almost degenerate eigenvalues close to 1. Therefore, Hankel matrices of the form

$$H_{jk} = \lambda d_{jk}(N) + \epsilon \mathfrak{H}_{jk}, \quad N = 2n + 2, \tag{31}$$

with $\mathfrak{H}_{jk} = h_{j+k}$ and $\epsilon \rightarrow 0$, have $n + 2$ eigenvalues close to λ .

A real symmetric $N \times N$ Hankel matrix h_{i+j} is determined by $N_t = 2N - 1$ parameters h_2, \dots, h_{2N} . Following the reasoning of the previous subsections, to obtain the small- s behavior of $P_n(s)$ one has to calculate the number of independent variables, apart from those that do not affect differences between eigenvalues. For matrices of the form close to the identity matrix as in (9) all eigenvalues are on the order of ϵ

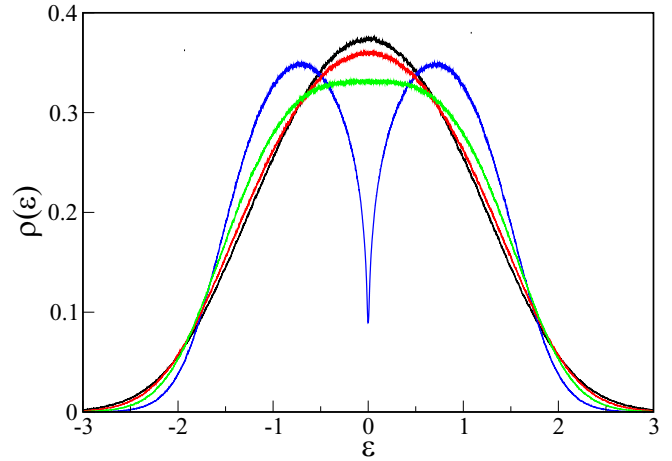


FIG. 2. Mean normalized densities $\bar{\rho}(\epsilon)$ for different classes of structured matrices. From top to bottom at $\epsilon = 0$: real and complex Toeplitz (black), independent real Toeplitz-plus-Hankel (red), independent complex Toeplitz-plus-Hankel (green), and Hankel (blue).

around λ . By contrast, in the case of matrices (31) there are certain \mathfrak{H} 's such that deviations of perturbed eigenvalues are on the order of ϵ^2 around λ . As we are looking for $P_n(s)$ only at the lowest order on s these “almost-zero modes” will give higher-order contribution and have to be excluded from the counting of independent variables.

Since $d(N)^2 = \mathbb{1}$ is the identity matrix, the square of matrix (31) is $H^2 = \lambda^2 \mathbb{1} + \lambda \epsilon [d(N)\mathfrak{H} + \mathfrak{H}d(N)] + \epsilon^2 \mathfrak{H}^2$. If the anticommutator of matrices $d(N)$ and \mathfrak{H} is zero,

$$d(N)\mathfrak{H} + \mathfrak{H}d(N) = 0, \tag{32}$$

then eigenvalues of H are $\pm \lambda + O(\epsilon^2)$ and such matrices correspond to almost-zero modes, and perturbations \mathfrak{H} in the direction specified by Eq. (32) will not affect eigenvalue spacings (at lowest order). The requirement (32) leads to the following conditions:

$$\begin{aligned} h_k + h_{2N-k} &= 0, & 2 \leq k \leq N, \\ h_{N+k} + h_{2N-k} &= 0, & 1 \leq k \leq N. \end{aligned} \tag{33}$$

As a consequence, for $2 \leq k \leq N - 2$ we must have $h_k = h_{N+k} = -h_{2N-k} = -h_{N-k}$ (in particular, this fixes $h_{N/2} = 0$). For $k = N - 1$ we must have $h_{N-1} = -h_{N+1} = h_{2N-1}$. For $k = N$ we get $h_N = h_{2N} = 0$. The remaining free parameters are, thus, $h_2, h_3, \dots, h_{N/2-1}, h_{N-1}$ and, of course, λ . This gives in total $n + 1$ almost-zero modes, so that $q_n = N_t - n - 1 = 3n + 2$. For random Hankel matrices with independent elements we, thus, get the γ distribution (13) with

$$\gamma_n = 3n + 1. \tag{34}$$

An alternative, perhaps a more transparent way of understanding the origin of condition (34) is to note that for Hankel matrices the condition $h_k = h_{N+k}$ with $k = 2, \dots, N$, obtained below (34), defines the so-called Hankel circulant matrices, which can easily be diagonalized in Fourier space [cf. Eq. (60)]. It is plain that for Hermitian matrices $H_{ij} = h_{i+j}$

TABLE I. Values of γ_n for different types of Hermitian matrices with independent elements.

Matrix type	γ_n
Complex Toeplitz matrices	$2n + 1$
Special Toeplitz-plus-Hankel matrices	$2n + 1$
Hankel matrices	$3n + 1$
Real Toeplitz-plus-Hankel matrices	$3n + 1$
Complex Toeplitz-plus-Hankel matrices	$4n + 2$

of the form (31) with such a property eigenvalues are given by

$$\lambda_n = \begin{cases} \pm|\xi_n|, & n \neq \frac{1}{2}N, N, \\ \xi_n, & n = \frac{1}{2}N, N, \end{cases} \quad \xi_n = \sum_{r=1}^N \mathfrak{h}_{r+N} e^{-2\pi i r n / N}. \quad (35)$$

In the problem considered here one has $h_N = h_{2N} = \lambda$ [cf. (30)]. Therefore,

$$\xi_n = \lambda + \sum_{r=1}^{N-1} \mathfrak{h}_{r+N} e^{-2\pi i r n / N}. \quad (36)$$

In order that the modulus $|\xi_n|$ equals $\lambda + O(\mathfrak{h}^2)$, it is necessary that the sum in this equation be a pure imaginary for all $n \neq N/2, N$. This requires $\mathfrak{h}_{r+N} + \mathfrak{h}_{2N-r} = 0$, which gives back (34).

The heuristic results of this section are that for all matrix families given by Eq. (1) the n th nearest-neighbor distributions $P_n(s)$ should be well described by the γ distribution (13) with γ_n summarized in Table I.

III. OTHER SPECTRAL PROPERTIES

A. Level compressibility

A characteristic property of models with intermediate statistics is the nontrivial value of the level compressibility χ , which is determined through the limiting behavior of the variance of the number of eigenvalues (normalized to unit density) in an interval of length L . If $N(L)$ is the number of eigenvalues inside the interval L then,

$$\Sigma^2(L) \equiv \langle [N(L) - L]^2 \rangle \underset{L \rightarrow \infty}{\sim} \chi L, \quad (37)$$

where the average is taken over different realizations of random matrices. For the usual Wigner-Dyson random matrix ensembles $\chi = 0$ and for the Poisson distribution $\chi = 1$. For intermediate statistics it is argued [27,28] that

$$0 < \chi < 1. \quad (38)$$

The calculation of the number variance requires the knowledge of the two-point correlation function $R_2(s)$, determined as the probability that two eigenvalues are separated by a distance s . Since there is an arbitrary number of eigenvalues inside this interval, it is plain that it equals the sum over all nearest-neighbor distributions,

$$R_2(s) = \sum_{n=0}^{\infty} P_n(s). \quad (39)$$

The γ distributions proposed above for $P_n(s)$ are only approximations to unknown expressions and small errors hardly

visible in the nearest-neighbor distributions may lead to considerable deviations in the infinite sum for $R_2(s)$. Nevertheless, it is instructive to see what is the compressibility for a γ distribution.

The distribution $P_n(s)$ has the form $s^{\gamma_n} \exp[-(\gamma_n + 1)s/(n + 1)]$, where $\gamma_n = pn + k$ with p and k independent of n . For $n \gg 1$ it has its maximum at $s \approx n + 1$ [which coincides with its mean value $n + 1$ given by the normalization (8)]. A second-order expansion near this maximum gives a Gaussian with mean value $n + 1$ and variance $\approx n/p$. At large n the distribution can, thus, be approximated asymptotically by

$$P_n(s) = \frac{1}{\sqrt{2\pi \Sigma^2(n)}} \exp\left(-\frac{(s - n - 1)^2}{2\Sigma^2(n)}\right), \quad \Sigma^2(n) = \frac{n}{p}. \quad (40)$$

This formula can be reversed to determine the behavior of $P_n(s)$ as function of n at large fixed s ,

$$P_n(s) = \frac{1}{\sqrt{2\pi \Sigma^2(s)}} \exp\left(-\frac{(n - s)^2}{2\Sigma^2(s)}\right), \quad \Sigma^2(s) = \frac{s}{p}. \quad (41)$$

Therefore, from the definition (37) it follows that

$$\Sigma^2(L) \approx \int (n - L)^2 P_n(L) dn = \frac{L}{p}, \quad (42)$$

which means that for a γ distribution with $\gamma_n = pn + k$,

$$\chi = \frac{1}{p}. \quad (43)$$

In other words, if $P_n(s)$ at large n has exponential decrease as $\exp(-ps)$ then $\chi = 1/p$. Such a relation is also valid for all short-range plasma models discussed in Ref. [32] (cf. Appendix B).

B. Form factor

The compressibility can be recovered alternatively from the asymptotic behavior of the two-point correlation form factor as

$$\chi = \lim_{\tau \rightarrow 0} K(\tau), \quad (44)$$

where the form factor is the Fourier transform of the spectral two-point correlation function, defined as

$$K(\tau) = \int_{-\infty}^{\infty} R_2(s) e^{2\pi i \tau s} ds. \quad (45)$$

The Fourier transform (45) can be evaluated by introducing the Laplace transform of the sum (39), which yields

$$K(\tau) = 1 + 2 \operatorname{Re} g(2\pi i \tau), \quad (46)$$

where the function g is defined as

$$g(t) = \sum_{n=0}^{\infty} g_n(t), \quad (47)$$

with $g_n(t)$ the Laplace transform of $P_n(s)$. Assuming that $\gamma_n = pn + k$ with p and k independent on n one gets from (13)

that

$$\begin{aligned}
 g_n(t) &= \int_0^\infty P_n(s) e^{-ts} ds \\
 &= \left(1 + \frac{(n+1)t}{pn+k+1}\right)^{-pn-k-1} \\
 &\underset{n \rightarrow \infty}{\sim} \exp\left[-\frac{t(p-k-1)}{p+t}\right] \left(1 + \frac{t}{p}\right)^{-pn-k-1}. \quad (48)
 \end{aligned}$$

As the direct summation over n is singular it is convenient to reexpress $g(t)$ as the sum of two terms,

$$g(t) = f(t) + \exp\left(-\frac{t(p-k-1)}{p+t}\right) \sum_{n=0}^{\infty} \left(1 + \frac{t}{p}\right)^{-pn-k-1}, \quad (49)$$

where

$$\begin{aligned}
 f(t) &= \sum_{n=0}^{\infty} \left[\left(1 + \frac{(n+1)t}{pn+k+1}\right)^{-pn-k-1} \right. \\
 &\quad \left. - \left(1 + \frac{t}{p}\right)^{-pn-k-1} \exp\left(-\frac{t(p-k-1)}{p+t}\right) \right]. \quad (50)
 \end{aligned}$$

The function f has a finite limit at $t \rightarrow 0$ and verifies $f(0) = 0$. The second term in (48) is easily calculated and yields

$$g(t) = f(t) + \frac{\left(1 + \frac{t}{p}\right)^{p-k-1}}{\left(1 + \frac{t}{p}\right)^p - 1} \exp\left(-\frac{t(p-k-1)}{p+t}\right). \quad (51)$$

Whereas (47) diverges when evaluated numerically, the form (49) and (50) allows to obtain a theoretical prediction for the form factor using Eq. (46). This expression will be compared with numerical computations in the next section.

From the second term it follows that

$$g(t) \underset{t \rightarrow 0}{\sim} \frac{1}{t} - \frac{p-1}{2p} + O(t). \quad (52)$$

The behavior of $g(t)$ at small t yields using (46) $\chi \equiv K(0) = 1/p$, which coincides with the expression in Eq. (43).

IV. COMPARISON WITH NUMERICAL CALCULATIONS

We now turn to the numerical determination of the different correlation functions for the families of random matrices considered above. The ensembles are constructed by taking all independent real matrix elements of these matrices (or all real and imaginary parts for complex entries) as Gaussian random variables with zero mean and unit variance. The spectra were obtained by diagonalization of matrices with dimension $N = 2^{10}$, and for each family 20 000 realizations of random matrices were taken.

A. Mean density of eigenvalues

The most basic quantity that characterizes the spectrum of a matrix of size N is the density of eigenvalues, defined as

$$\bar{\rho}(E) = \frac{1}{N} \left\langle \sum_{j=1}^N \delta(E - E_j) \right\rangle, \quad (53)$$

where the average is taken over different realizations of random parameters.

It is well known that for the usual Wigner-Dyson random matrix ensembles the mean density of states follows the Wigner semicircle law. On the other hand, for real symmetric Toeplitz and Hankel matrices, it was shown in Refs. [46,47] that the mean densities (rescaled by \sqrt{N}) converge when $N \rightarrow \infty$ to nontrivial symmetric distributions depending only on the variance of matrix elements. To meaningfully compare mean densities of different matrix ensembles it is convenient to rescale them in such a way that

$$\int E^2 \bar{\rho}(E) dE = 1. \quad (54)$$

This can be achieved by rescaling energy levels as $\varepsilon = E/\sigma$ with $\sigma^2 = \langle \text{Tr}(M^2) \rangle / N$. For matrices (1) with independent entries of zero mean and unit variance, one readily gets that for large N the rescaling factor is $\sigma^2 = N$ for real symmetric Toeplitz matrices and Hankel matrices, $\sigma^2 = 2N$ for complex Toeplitz matrices and real Toeplitz-plus-Hankel matrices with independent entries, and $\sigma^2 = 3N$ for complex Toeplitz-plus-Hankel matrices. The rescaled mean densities are presented in Fig. 2.

B. Nearest-neighbor distributions

In order to compare numerical data with universal analytic predictions, we need to perform what is known as an ‘‘unfolding’’ procedure. Assuming that eigenvalues are ordered $E_{j+1} \geq E_j$, unfolded eigenvalues e_j are defined as

$$e_j = \bar{N}(E_j), \quad (55)$$

where $\bar{N}(E)$ is the cumulative mean density,

$$\bar{N}(E) = \int_{-\infty}^E \bar{\rho}(E') dE'. \quad (56)$$

The unfolded eigenvalues have unit mean density. Nearest-neighbor distributions $P_n(s)$ are then calculated from a small interval of the unfolded spectrum around the maximum of $\bar{\rho}(E)$. In practice we took an interval containing 1/4 of the total number of levels around the center of the spectrum. For Hankel matrices, however, because of the unusual two-peak form of the density (see Fig. 2), eigenvalues were taken around the right peak only.

The results for nearest-neighbor distributions $P_n(s)$ with $0 \leq n \leq 5$ are presented in Fig. 3 for complex Toeplitz matrices and for special $T \pm H$ matrices together with the theoretical γ distributions (13). The same quantities for Hankel matrices and for real and complex independent Toeplitz-plus-Hankel matrices are plotted in Fig. 4. The theoretical distributions (13) agree quite well with numerical calculations, despite the fact that these formulas have no free parameters. Note that numerically calculated spectral correlation functions of Hankel and real Toeplitz-plus-Hankel matrices are close to each other (see Fig. 4 top), although their spectral densities, plotted in Fig. 2, are very different.

In order to further improve the formulas for $P_n(s)$, one can replace the term s^{ν} in Eq. (13) by a polynomial in s as happens in the short-range plasma model [32]. This is briefly discussed in Appendix B. A drawback of such an approach is that normalization of the expressions lead to quite cumbersome formulas. We found that the simplest way to improve

TABLE II. Values of fitted γ_n with $n = 0, \dots, 5$ for different matrices.

Matrix type	γ_0	γ_1	γ_2	γ_3	γ_4	γ_5
Complex Toeplitz matrices	1.12	3.28	5.45	7.66	9.88	12.12
Special Toeplitz-plus-Hankel matrices	0.86	2.86	4.95	7.08	9.24	11.42
Hankel matrices	1.17	3.77	6.48	9.27	12.09	14.96
Real Toeplitz-plus-Hankel matrices	1.22	3.96	6.83	9.81	12.84	15.92
Complex Toeplitz-plus-Hankel matrices	2.00	5.58	9.33	13.20	17.13	21.08

our surmise for $P_n(s)$ is to use the same γ distribution (13) with normalization (14) but with a value of γ_n obtained from a one-parameter fit of the data (the only free parameter being γ_n). Surprisingly, such *ad hoc* fits work very well. The results are displayed in Figs. 3 and 4, and the fitting curves in the bulk entirely go through numerical points. In the insets of these figures we compare the fitted values of γ_n , given in Table II with the predictions of Table I.

C. Two-point correlation form factor

The two-point correlation form factor $K(\tau)$ is the Fourier transform of the spectral two-point correlation function $R_2(s)$. It can be expressed in terms of the unfolded spectrum as

$$K(\tau) = \frac{1}{N} \left\langle \left| \sum_{j=1}^N e^{2\pi i e_j \tau} \right|^2 \right\rangle \quad (57)$$

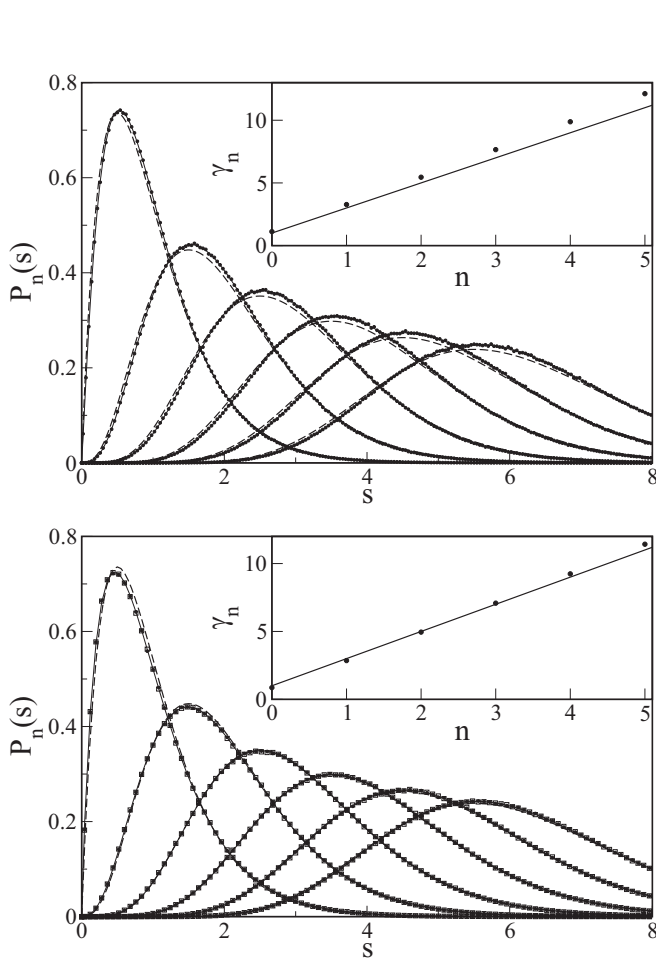


FIG. 3. $P_n(s)$ for $0 \leq n \leq 5$ for (top) complex Toeplitz matrices (open black squares) and (bottom) special $T + H$ matrices (filled black circles) and special $T - H$ matrices (open black squares) given by (16). Black dashed lines are γ distributions (13) with $\gamma_n = 2n + 1$ (semi-Poisson distribution). Black solid lines are γ distributions fitted with a single fitting parameter γ_n . The corresponding fitted values of γ_n are given in Table II and plotted in the insets (filled black circles) together with the semi-Poisson prediction $\gamma_n = 2n + 1$ (solid black line).

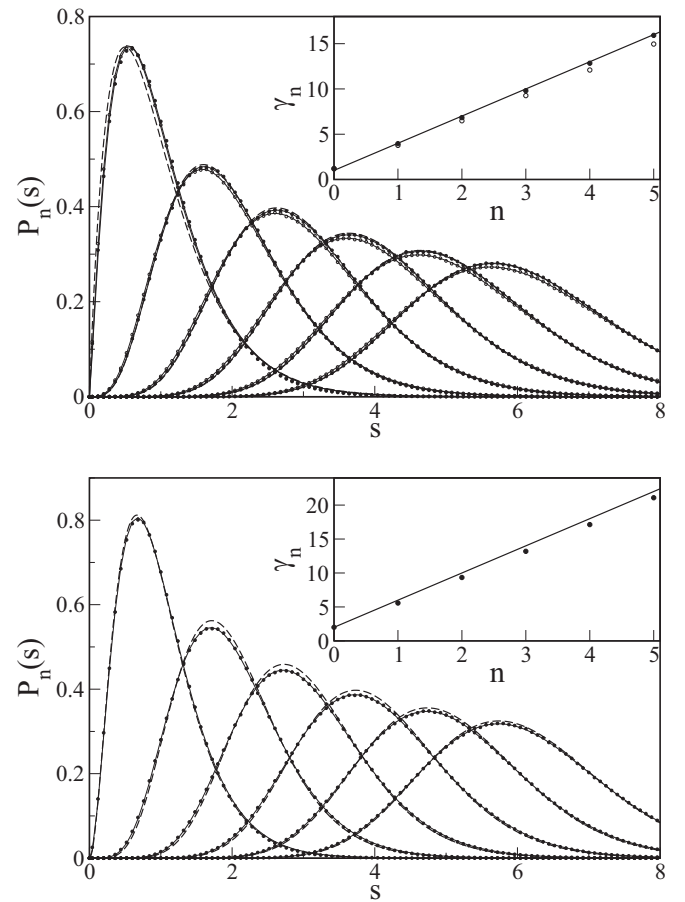


FIG. 4. (Top) $P_n(s)$ for $0 \leq n \leq 5$ for Hankel matrices (open black circles) and real Toeplitz-plus-Hankel matrices (filled black circles). The black dashed lines are the γ distributions (13) with $\gamma_n = 3n + 1$. The inset displays the values of γ_n obtained by a one-parameter fit (same symbols as in the main panel) and given in Table II, and the black solid line is the prediction $\gamma_n = 3n + 1$. (Bottom) The same for complex Toeplitz-plus-Hankel matrices (filled black circles). The black dashed lines are the γ distributions (13) with $\gamma_n = 4n + 2$, and the black solid lines are the γ distributions obtained by a one-parameter fit. The inset shows the fitted values of γ_n (filled black circles) and the prediction $\gamma_n = 4n + 2$.

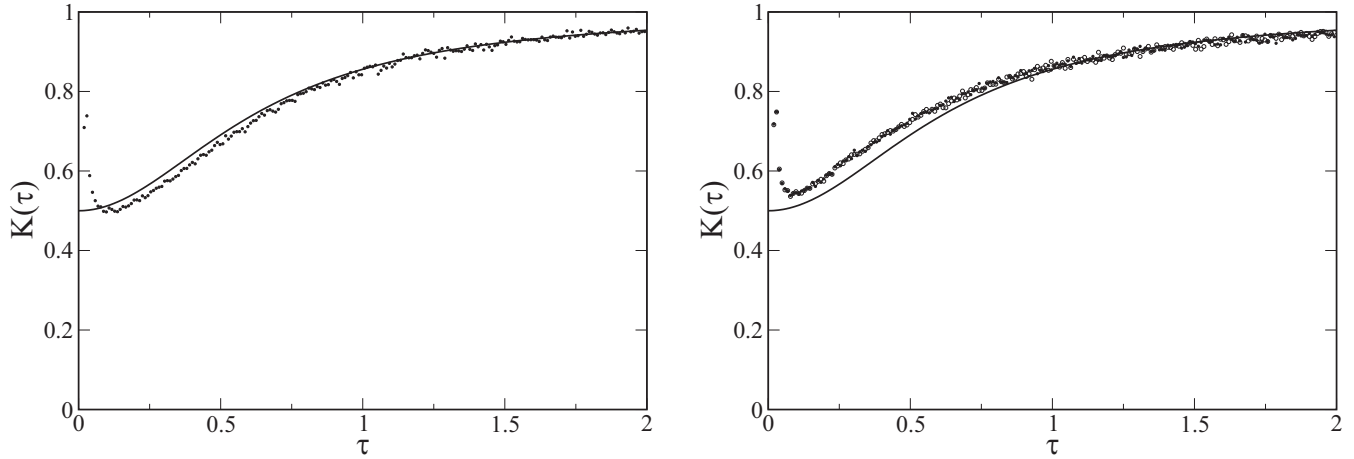


FIG. 5. The form factor of (left) complex Toeplitz matrices (filled black circles), (right) special $T + H$ matrices (filled black circles), and special $T - H$ matrices (open black circles). Circles are the numerical computations using (57), and the solid black line is the form factor of the γ distribution with $\gamma_n = 2n + 1$ (i.e., the semi-Poisson distribution) calculated from (49) and (50).

(see, e.g., Ref. [48]). The form factor of complex Toeplitz matrices and special $T \pm H$ matrices (16), computed numerically from (56), is displayed in Fig. 5. In Fig. 6(a) we plot the same function for Hankel and real independent Toeplitz-plus-Hankel matrices and in Fig. 6(b) for complex independent Toeplitz-plus-Hankel matrices. The form factors for $\gamma_n = 2n + 1, 3n + 1, 4n + 2$, calculated from the above formula (45) are presented in Figs. 5 and 6 together with the exact form factors of corresponding short-range plasma models presented in Appendix B.

It is known that numerical calculation of the spectral compressibility from finite-dimensional matrices is subtle. The point is that the compressibility is defined either from the large- L behavior of the number variance (37) or from the limiting value of the form factor at small argument (44). In such definitions it is implicitly assumed that the limit $N \rightarrow \infty$ is taken first, but in numerics one fixes the matrix dimension.

This inevitable inversion of the limits is responsible for the sudden increase in $K(\tau)$ evident in the above figures. The same phenomenon is clearly seen even in (57) where formally $K(0) = N \rightarrow_{N \rightarrow \infty} \infty$ [cf. also the discussion after Eq. (49)]. More and more realizations of random parameters are needed to get correctly the limiting value $K(0)$. This is illustrated in the inset of Fig. 6. The discussion of different interpolation procedures is beyond the scope of the paper. Nevertheless, from Figs. 5 and 6 it is clear that the γ distribution prediction, $K(0) = 1/p$ with p from Table I, is in a reasonable agreement with numerical calculations.

D. Fractal dimensions

Previous sections have shown that spectral statistics of Toeplitz and Hankel matrices, or their sums, are of intermediate type. Such a behavior of spectral fluctuations has been

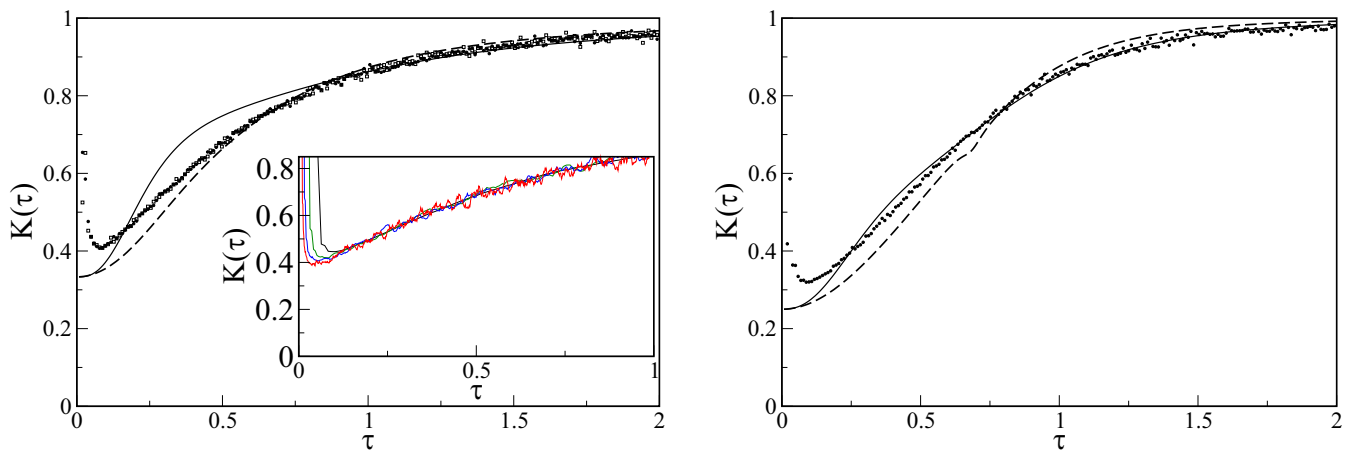


FIG. 6. (left) The form factor of Hankel matrices (filled black circles) and independent real Toeplitz-plus-Hankel matrices (open black squares). The inset: evolution of the form factor near the origin for Hankel matrices with increasing matrix dimension $N = 2^n$ with (from right to left at small τ) $n = 10$ (black), $n = 11$ (green), $n = 12$ (blue), and $n = 13$ (red). (right) The form factor of independent complex Toeplitz-plus-Hankel matrices (filled black circles). The solid black line is the form factor of γ distribution with: (left) $\gamma_n = 3n + 1$, and (right) $\gamma_n = 4n + 2$ calculated from (49) and (50). The dashed line is the form factor for short-range plasma model with the same value of γ_n , given by (B9) and (B10).

associated with multifractal properties of eigenstates [33–35]. Multifractals are objects that display fluctuations at all scales and are characterized by the existence of a whole range of fractal dimensions.

Contrary to eigenvalues, eigenvectors (and, thus, multifractality and fractal dimensions) depend on the chosen basis. For models with intermediate-type statistics eigenfunctions are typically fully extended in coordinate space but multifractal in Fourier space. We, thus, introduce eigenfunctions $\hat{\Psi}_p(E)$, defined as the Fourier transform of eigenvectors $\Psi_j(E)$ through the usual expression,

$$\hat{\Psi}_p(E) = \frac{1}{\sqrt{N}} \sum_{j=1}^N e^{2\pi i j p / N} \Psi_j(E), \quad (58)$$

where $\Psi_j(E)$ is the eigenvector corresponding to the eigenvalue E and it is assumed that this vector is normalized as $\sum_{j=1}^N |\Psi_j(E)|^2 = 1$. These functions could be also calculated by the diagonalization of Fourier transform of matrices (1). The Fourier transform of the Toeplitz matrix is given in Ref. [23]. For Hankel matrices one gets

$$\begin{aligned} \hat{H}_{mn} &= \frac{1}{N} \sum_{j,k=1}^N h_{j+k} e^{2\pi i (km - jn) / N} \\ &= \xi_n d_{mn}(N) - [1 - d_{mn}(N)] \\ &\quad \times \left[\frac{\eta_n}{1 - e^{-2\pi i (m+n) / N}} + \frac{\eta_m^*}{1 - e^{2\pi i (m+n) / N}} \right]. \end{aligned} \quad (59)$$

Here matrix $d_{mn}(N)$ was defined in (30) and

$$\begin{aligned} \xi_n &= \frac{1}{N} \sum_{r=2}^N (h_r - h_{r+N})(r-1) e^{-2\pi i r n / N} + \sum_{r=1}^N h_{r+N} e^{-2\pi i r n / N}, \\ \eta_n &= \frac{1}{N} \sum_{r=2}^N (h_r - h_{r+N}) e^{-2\pi i r n / N}. \end{aligned} \quad (60)$$

In order to define multifractal dimensions one calculates the moments of eigenvectors and their scaling with matrix dimension (see, e.g., Ref. [49] and references therein),

$$\left\langle \sum_{p=1}^N |\hat{\Psi}_p(E)|^{2q} \right\rangle \underset{N \rightarrow \infty}{\sim} C N^{-\tau(q)}. \quad (61)$$

The average in the above expression is taken over different realizations of random parameters and over all eigenvalues in a small energy window around E . The exponent $\tau(q)$ determines the dependence of the q th moment with N . If an eigenvector has a small number of large components then $\tau(q) = 0$. If all components are of comparable magnitudes then, from normalization, $|\Psi_j(E)|^2 \sim N^{-1}$, and, thus, $\tau(q) = q - 1$. The ratios,

$$D_q = \frac{\tau(q)}{q-1} \quad (62)$$

are called (multi)fractal dimensions, and they are the main characteristics of statistical properties of eigenvectors. For localized states $D_q = 0$ and for fully extended states $D_q = 1$. Systems for which D_q differs from these extreme values and depend on q are called multifractal.

For the ensembles of random matrices considered here, eigenvectors $\Psi_j(E)$ were obtained by exact diagonalization and Fourier transformed according to (58). The exponents $\tau(q)$ were extracted from a linear fit of the logarithm of moments (61) as a function of $\ln N$, for data from $N = 2^7$ (8000 realizations) to $N = 2^{12}$ (200 realizations) in a small window of eigenvalues around the maximum of the density. The numerical results are displayed in Fig. 7. A first observation is that for all the matrix ensembles considered here, fractal dimensions are nontrivial (i.e., different from 0 and 1). As was the case for the spectra, fractal dimensions of Hankel and independent real Toeplitz-plus-Hankel matrices are very close to each other. Although for $q < -1$ they seem to deviate, big numerical uncertainties in this region due to small wave function values taken at a negative power, do not permit to get a clear-cut conclusion.

There are practically no general results for fractal dimensions. In Ref. [50], based on the nonlinear σ model, it was conjectured that the anomalous dimensions defined by

$$\Delta_q = (D_q - 1)(q - 1) \quad (63)$$

should satisfy the following symmetry relation,

$$\Delta_q = \Delta_{1-q}. \quad (64)$$

In the inset of Fig. 7, values of Δ_q and Δ_{1-q} are plotted for Toeplitz, Hankel, and complex Toeplitz-plus-Hankel matrices. It is clear that the relation (64) is valid only in the interval $|q| < 1$ where fractal dimensions are practically linear. At larger values of q this relation numerically breaks down.

The quantity D_1 has a special importance as it is a kind of eigenfunction entropy,

$$\sum_{p=1}^N |\hat{\Psi}_p|^2 \ln |\hat{\Psi}_p|^2 \underset{N \rightarrow \infty}{\sim} -D_1 \ln N. \quad (65)$$

In Ref. [51] it was conjectured that

$$D_1 + \chi = 1, \quad (66)$$

where χ is the level compressibility discussed in Sec. III A. Numerically one finds that for complex Toeplitz matrices $D_1 \approx 0.52$ for special $T \pm H$ matrices $D_1 \approx 0.52$, for Hankel matrices $D_1 \approx 0.65$, for real Toeplitz-plus-Hankel matrices $D_1 \approx 0.67$, and for complex Toeplitz-plus-Hankel matrices $D_1 \approx 0.75$. These numerical values are quite close to the theoretical values of $1/2$, $2/3$, and $3/4$ expected from Eqs. (43) and (66), which indicates that the conjecture (66) (approximately) extends to the all the above random matrix ensembles.

V. SUMMARY

Toeplitz, Hankel, and Toeplitz-plus-Hankel matrices are probably the oldest and the best investigated classes of matrices. Although it was known for a long time that these matrices are examples of low-complexity matrices, the investigation of statistical properties of such matrices with very irregular (which may and will be naturally substituted by random) elements did not attract wide attention.

In the present paper such Hermitian matrices with independent and identically distributed random elements were investigated in detail. The main spectral correlation functions

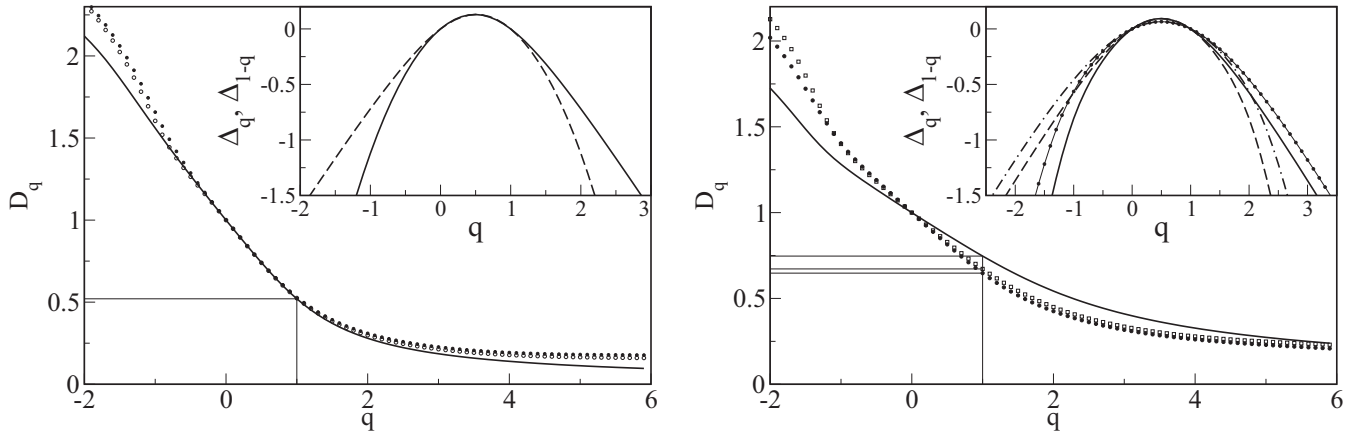


FIG. 7. Fractal dimensions in the Fourier space for (left) complex Toeplitz matrices (solid black line) and for special $T + H$ matrices (filled black circles) and $T - H$ matrices (open black circles) given by (16) and (right) Hankel matrices (filled black circles), independent real Toeplitz-plus-Hankel matrices (open black squares), and independent complex Toeplitz-plus-Hankel matrices (solid black line). Points corresponding to D_1 are indicated by thin straight lines. In the insets Δ_q and Δ_{1-q} are plotted together for (left) complex Toeplitz matrices (solid line is Δ_q and dashed line is Δ_{1-q}) and for (right) Hankel matrices (Δ_q is indicated by solid line and Δ_{1-q} by dashed line), and for independent complex Toeplitz-plus-Hankel matrices (Δ_q is indicated by filled black circles connected by a thin line and Δ_{1-q} by dashed-dot line).

were calculated using large matrix dimensions and large number of realizations. Special attention was given to the careful determination of nearest-neighbor distributions of these matrices. It is demonstrated that these families of matrices display level repulsion at small distances, as for usual Wigner-Dyson ensembles of random matrices, but their nearest-neighbor distributions decrease exponentially at large argument, contrary to the Wigner-Dyson ensembles where they have Gaussian tails. Combination of these two properties is the characteristic feature of the so-called intermediate spectral statistics observed until now only in rare special systems, such as the Anderson model at the point of metal-insulator transition, certain pseudointegrable billiards, intermediate kicked quantum maps, and matrix ensembles related with Lax matrices of integrable models.

The form factor (the Fourier transform of the two-point spectral correlation function) is a key characteristic of spectral statistics, and its value at 0, the level compressibility, provides a signature of the nature of these statistics: It takes the value of 0 for the Wigner-Dyson ensembles, 1 for the Poisson statistics, and an intermediate value for intermediate statistics. For all matrices considered here the form factors were calculated numerically, and it was demonstrated that they are different from standard random matrix ensembles. In particular, the data indicate that the spectral compressibility of Toeplitz, Hankel, and Toeplitz-plus-Hankel matrices is nontrivial, which is another characteristic feature common to all known intermediate-type statistics. Moreover, numerical calculations of statistical properties of the corresponding eigenvectors show that their fractal dimensions are also nontrivial (i.e., different from 0 or 1) for all considered matrices, which shows that such eigenfunctions are multifractal.

Exact analytic results for such statistical distributions are nonexistent. Here we developed a simple heuristic method to get approximate formulas of the nearest-neighbor distributions for the considered classes of random matrices. They

correspond to the normalized γ distribution with parameter γ_n given in Table I. The obtained expressions have no free parameter and approximate well the numerical results. Adding a single fitting parameter (the parameter γ of the γ distribution) gives almost perfect agreement with the data in the bulk. Therefore, in the same way as the celebrated Wigner surmise, and because of their simplicity, our formulas can serve as approximations to unknown distributions. We also observed that numerically calculated correlation functions for Hankel random matrices and independent real Toeplitz-plus-Hankel matrices are surprisingly close to each other, although their spectral densities are very different.

The fact that all low-complexity matrices discussed in the paper have this type of statistics clearly shows that intermediate statistics are more widely spread than was considered before and opens new perspectives in random matrix theory. As this type of matrices pervades all branches of physical and mathematical sciences, it is an important challenge to derive analytically correlation functions in these models.

APPENDIX A: DISPLACEMENT STRUCTURE FOR TOEPLITZ, HANKEL, AND TOEPLITZ-PLUS-HANKEL MATRICES

Let Z be the $n \times n$ matrix,

$$Z_{jk} = \delta_{j-k-1}. \tag{A1}$$

This matrix shifts any matrix M as

$$\begin{aligned} (ZM)_{ij} &= M_{i-1,j} \Theta(i-1) \longrightarrow \text{shift down,} \\ (Z^T M)_{ij} &= M_{i+1,j} \Theta(n-i) \longrightarrow \text{shift up,} \\ (MZ)_{ij} &= M_{i,j+1} \Theta(n-j) \longrightarrow \text{shift left,} \\ (MZ^T)_{ij} &= M_{i,j-1} \Theta(j-1) \longrightarrow \text{shift right,} \end{aligned} \tag{A2}$$

where $\Theta(n) = 1$ for $n > 0$ and $\Theta(n) = 0$ for $n \leq 0$. When applied to a Toeplitz matrix $T_{jk} = t_{j-k}$ with $j, k = 1, \dots, n$,

the operation ZTZ^\dagger shifts it along the main diagonal by one unit (hence, the name displacement structure),

$$(ZTZ^T)_{ij} = t_{i-j}\Theta(i-1)\Theta(j-1). \quad (A3)$$

Therefore, all terms in the displacement operator $\nabla_{Z,Z^T}(T) = T - ZTZ^T$ cancel except for $i, j = 1$, and

$$T - ZTZ^T = \begin{bmatrix} t_0 & t_{-1} & t_{-2} & \cdots & t_{1-n} \\ t_1 & 0 & 0 & \cdots & 0 \\ \vdots & \ddots & \ddots & \ddots & \vdots \\ t_{n-2} & 0 & \cdots & 0 & 0 \\ t_{n-1} & 0 & \cdots & 0 & 0 \end{bmatrix}. \quad (A4)$$

Consequently, the displacement rank for any Toeplitz matrix is at most 2.

For Hankel matrices, $H_{jk} = h_{j+k}$ with $j, k = 1, \dots, n$ it is convenient to use the operation,

$$(ZH - HZ^T)_{ij} = h_{i-1+j}\Theta(i-1) - h_{i+j-1}\Theta(j-1). \quad (A5)$$

All terms in the displacement operator $\Delta_{Z,Z^T}(H) = ZH - HZ^T$ cancel except for $i, j = 1$,

and

$$ZH - HZ^T = \begin{bmatrix} 0 & -h_2 & -h_3 & \cdots & -h_n \\ h_2 & 0 & 0 & \cdots & 0 \\ \vdots & \ddots & \ddots & \ddots & \vdots \\ h_{n-1} & 0 & \cdots & 0 & 0 \\ h_n & 0 & \cdots & 0 & 0 \end{bmatrix}. \quad (A6)$$

Therefore, the displacement rank of a Hankel matrix is also at most 2.

For a Toeplitz-plus-Hankel matrix, $(T + H)_{ij} = t_{i-j} + h_{i+j}$ with $j, k = 1, \dots, n$, Eq. (A3) yields the identities,

$$[Z(T + H)]_{ij} = (t_{i-j-1} + h_{i+j-1})\Theta(i-1), \quad (A7)$$

$$[Z^T(T + H)]_{ij} = (t_{i-j+1} + h_{i+j+1})\Theta(n-i), \quad (A8)$$

$$[(T + H)Z]_{ij} = (t_{i-j-1} + h_{i+j+1})\Theta(n-j), \quad (A9)$$

$$[(T + H)Z^T]_{ij} = (t_{i-j+1} + h_{i+j-1})\Theta(j-1). \quad (A10)$$

Defining the displacement operator by [8]

$$\Delta_{A,A}(T + H) = A(T + H) - (T + H)A, \quad A = Z + Z^T, \quad (A11)$$

all terms in $\Delta_{A,A}(T + H)$ cancel except the boundary terms with $i = 1, n$ and $j = 1, n$, so that it has the block structure,

$$\Delta_{A,A}(T + H) = \begin{bmatrix} t_1 - t_{-1} & -(t_{-j} + h_j)_{j=2}^{n-1} & h_{2+n} - h_n \\ (t_i + h_i)_{i=2}^{n-1} & (0)_{i,j=2}^{n-1} & (t_{i-n+1} + h_{i+n-1})_{i=2}^{n-1} \\ h_n - h_{2+n} & -(t_{n-j-1} + h_{n+j+1})_{j=2}^{n-1} & t_{-1} - t_1 \end{bmatrix}. \quad (A12)$$

In general, the displacement rank of a Toeplitz-plus-Hankel matrix is at most 4.

APPENDIX B: SHORT-RANGE PLASMA MODELS

The usual semi-Poisson distribution corresponds to the case where only the nearest levels (from the ordered set) interact by the factor $f(\lambda, \lambda') = |\lambda' - \lambda|^\beta$. For this model all correlation functions are known [32,52]. $P_n(s)$ are γ distributions with $\gamma_n = 2n + 1$ for $\beta = 1$ and $\gamma_n = 3n + 2$ for $\beta = 2$. The two-point correlation form factors are given by the following formulas:

$$K(\tau) = \frac{2 + \pi^2\tau^2}{4 + \pi^2\tau^2}, \quad K(0) = \frac{1}{2}, \quad \beta = 1, \quad (B1)$$

$$K(\tau) = 1 - \frac{486}{729 + 108\pi^2\tau^2 + 16\pi^4\tau^4}, \quad K(0) = \frac{1}{3}, \quad \beta = 2. \quad (B2)$$

But one can also consider the case when there exists also an interaction with the next-to-nearest neighbors. Here we consider two such models. The first one has been discussed in detail in Ref. [32]. It corresponds to a model where the nearest and next-to-nearest levels interact by the same interaction: If $\lambda_1 < \lambda_2 < \lambda_3$ is any triple of nearest levels then they have the usual interaction with $\beta = 1$,

$$|\lambda_3 - \lambda_2||\lambda_2 - \lambda_1||\lambda_3 - \lambda_1|. \quad (B3)$$

It is easy to see that at small arguments the nearest-neighbor distributions have s^{γ_n} behavior with $\gamma_n = 3n + 1$. The calculations in Ref. [32] give

$$P_0(s) = \frac{9}{2}(3 - \sqrt{6})s \exp(-3s) \left(1 + \frac{\sqrt{6}}{2}s\right)^2, \\ P_1(s) = \frac{3^4}{2^3}(5\sqrt{6} - 12)s^4 \exp(-3s) \left(1 + \frac{\sqrt{6}}{2}s + \frac{3}{10}s^2\right), \\ P_2(s) = \frac{3^8}{7 \times 5 \times 2^5}(27 - 11\sqrt{6})s^7 \exp(-3s) \left(1 + \frac{11}{36}\sqrt{6}s + \frac{s^2}{8}\right). \quad (B4)$$

The second model is chosen in such a way that the nearest levels interact with $\beta = 2$ but the next-to-nearest levels interact with $\beta = 1$,

$$|\lambda_3 - \lambda_2|^2 |\lambda_2 - \lambda_1|^2 |\lambda_3 - \lambda_1|. \tag{B5}$$

In this case,

$$P_n(s) \underset{s \rightarrow 0}{\sim} s^{\gamma_n}, \quad \gamma_n = 4n + 2. \tag{B6}$$

Such a case has not been considered in Ref. [32] but the calculations can be performed similarly as in the first model and the results are the following:

$$P_0(s) = 2^5 (2 - \sqrt{3}) s^2 \exp(-4s) \left(1 + \frac{2\sqrt{3}}{3} s \right)^2, \tag{B7}$$

$$P_1(s) = \frac{2^{11}}{5 \times 3^2} (7\sqrt{3} - 12) s^6 \exp(-4s) \left(1 + \frac{2\sqrt{3}}{3} s + \frac{2}{7} s^2 \right), \tag{B7}$$

$$P_2(s) = \frac{2^{14} \times 13}{7 \times 5^2 \times 3^4} (26 - 15\sqrt{3}) s^{10} \exp(-4s) \left(1 + \frac{60\sqrt{3}}{143} s + \frac{4}{33} s^2 \right). \tag{B8}$$

Similar formulas can be derived for the two-point correlation form factors. The direct calculations show that the Laplace transform of the form factor has the following form:

$$g_2(t) = \frac{9}{4(3+t)} \left[\frac{(6+t)^2}{(3+t)^3 - 3^3} + \frac{t^2(5-2\sqrt{6})}{(3+t)^3 + 3^3(5-2\sqrt{6})} \right], \quad \gamma_n = 3n + 1, \tag{B9}$$

$$g_2(t) = \frac{16}{4+t} \left[\frac{(8+t)^2}{(4+t)^4 - 4^4} + \frac{t^2(7-4\sqrt{3})}{(4+t)^4 + 4^4(7-4\sqrt{3})} \right], \quad \gamma_n = 4n + 2. \tag{B10}$$

The two-point form factor is related with the Laplace transform by (46). The values of the form factor at zero are 1/3 for the first model and 1/4 for the second one, in accordance with results of Sec. III A. The corresponding curves are presented in Fig. 6.

[1] V. Y. Pan, Z. Q. Chen, and A. Zheng, The complexity of the algebraic eigenproblem, in *Proceedings of the Thirty-First Annual ACM Symposium on Theory of Computing (STOC'99)*, Atlanta, GA, 1999 (ACM Press, New York, 1999), p. 507.

[2] D. Coppersmith and S. Winograd, Matrix multiplication via arithmetic progressions, *J. Symb. Comp.* **9**, 251 (1990).

[3] F. Le Gall, Powers of tensors and fast matrix multiplication, in *Proceedings of the 39th International Symposium on Symbolic and Algebraic Computation (ISSAC'14)* (ACM, New York, 2014), p. 296.

[4] J. Alman and V. V. Williams, A refined laser method and faster matrix multiplication, in *Proceedings of the 2021 ACM-SIAM Symposium on Discrete Algorithms (SODA)* (SIAM, Philadelphia, 2021), pp. 522–539.

[5] T. Kailath, S.-Y. Kung, and M. Morf, Displacement ranks of matrices and linear equations, *J. Math. Anal. Appl.* **68**, 395 (1979).

[6] T. Kailath, A. Viera, and M. Morf, Inverses of Toeplitz operators, innovations, and orthogonal polynomials, *SIAM Rev.* **20**, 106 (1978).

[7] M. Morf, Doubling algorithms for Toeplitz and related equations, in *Proceedings of the IEEE International Conference on Acoustics, Speech, and Signal Processing (ICASSP'80)*, Denver, CO, 1980 (IEEE, New York, 1980), p. 954.

[8] G. Heinig, P. Jankowski, and K. Rost, Fast inversion algorithms of Toeplitz-plus-Hankel matrices, *Numer. Math.* **52**, 665 (1988).

[9] V. Y. Pan, *Structured Matrices and Polynomials, Unified Superfast Algorithms* (Birkhäuser, Basel, Switzerland, 2001).

[10] H. Hankel, in *Über eine Besondere Classe der Symmetrischen Determinanten*, edited by W. F. Kaestner (Göttingen, 1861).

[11] O. Toeplitz, Zur Theorie der Quadratischen und Bilinearen Formen von Wendlichvielen Veränderlichen, 1. Teil: Theorie der L-Formen, *Math. Ann.* **70**, 351 (1911).

[12] U. Grenander and G. Szegő, *Toeplitz Forms and Their Applications* (University of California Press, Berkeley, CA, 1958).

[13] I. S. Iohvidov, *Hankel and Toeplitz Matrices and Forms: Algebraic Theory* (Birkhäuser, Boston, 1982).

[14] A. Böttcher and B. Silbermann, *Introduction to Large Truncated Toeplitz Matrices* (Springer, New York, 1999).

[15] V. Peller, *Hankel Operators and Their Applications* (Springer-Verlag, New York, 2011).

[16] P. Deift, A. Its, and I. Krasovsky, Asymptotics of Toeplitz, Hankel, and Toeplitz plus Hankel determinants with Fisher-Hartwig singularities, *Ann. Math.* **174**, 1243 (2011).

[17] P. Deift, A. Its, and I. Krasovsky, Toeplitz matrices and Toeplitz determinants under the impetus of the Ising model. Some history and some recent results, *Commun. Pure Appl. Math.* **66**, 1360 (2013).

[18] I. Krasovsky, Aspects of Toeplitz determinants, in *Random Walks, Boundaries and Spectra*, edited by D. Lenz, F. Sobieczky, and W. Woess, Progress in Probability Vol. 64 (Springer, Basel, 2011), pp. 305–324.

[19] N. Levinson, The Wiener RMS (root mean square) error criterion in filter design and prediction, *J. Math. Phys.* **25**, 261 (1947).

- [20] W. F. Trench, An algorithm for the inversion of finite Toeplitz matrices, *SIAM J. Appl. Math.* **12**, 515 (1964).
- [21] W. F. Trench, Numerical solution of the eigenvalues problem for hermitian Toeplitz matrices, *SIAM J. Matrix Anal. Appl.* **10**, 135 (1989).
- [22] W. F. Trench, An algorithm for the inversion of finite Hankel matrices, *SIAM J. Appl. Math.* **13**, 1102 (1965).
- [23] E. Bogomolny, Spectral statistics of random Toeplitz matrices, *Phys. Rev. E* **102**, 040101(R) (2020).
- [24] O. Bohigas, M. J. Giannoni, and C. Schmit, Characterization of Chaotic Quantum Spectra and Universality of Level Fluctuation Laws, *Phys. Rev. Lett.* **52**, 1 (1984).
- [25] M. L. Mehta, *Random Matrices*, 3rd ed. (Academic Press, New York, 2004).
- [26] M. V. Berry and M. Tabor, Level clustering in the regular spectrum, *Proc. R. Soc. London, Ser. A* **356**, 375 (1977).
- [27] B. I. Shklovskii, B. Shapiro, B. R. Sears, P. Lambrianides, and H. B. Shore, Statistics of spectra of disordered systems near the metal-insulator transition, *Phys. Rev. B* **47**, 11487 (1993).
- [28] B. L. Altshuler, I. K. Zharekeshev, S. A. Kotochigava, and B. I. Shklovskii, Repulsion between levels and the metal-insulator transition, *JETP* **67**, 625 (1988).
- [29] E. B. Bogomolny, U. Gerland, and C. Schmit, Models of intermediate spectral statistics, *Phys. Rev. E* **59**, R1315(R) (1999).
- [30] J. Wiersig, Spectral properties of quantized barrier billiards, *Phys. Rev. E* **65**, 046217 (2002).
- [31] O. Giraud, J. Marklof, and S. O’Keefe, Intermediate statistics in quantum maps, *J. Phys. A* **37**, L303 (2004).
- [32] E. Bogomolny, U. Gerland, and C. Schmit, Short-range plasma model for intermediate spectral statistics, *Eur. Phys. J. B* **19**, 121 (2001).
- [33] F. Wegner, Inverse participation ratio in $2 + \epsilon$ dimensions, *Z. Phys. B* **36**, 209 (1980).
- [34] H. Aoki, Critical behavior of extended states in disordered systems, *J. Phys. C* **16**, L205 (1983).
- [35] C. Castellani and L. Peliti, Multifractal wavefunction at the localisation threshold, *J. Phys. A* **19**, L429 (1986).
- [36] E. Bogomolny and O. Giraud, Perturbation approach to multifractal dimensions for certain critical random matrix ensembles, *Phys. Rev. E* **84**, 036212 (2011).
- [37] *Statistical Theories of Spectra: Fluctuations*, edited by C. E. Porter (Academic Press, New York, 1965).
- [38] M. Jimbo, T. Miwa, Y. Môri, and M. Sato, Density matrix of an impenetrable Bose gas and the fifth Painlevé transcendent, *Physica D* **1**, 80 (1980).
- [39] A. M. Odlyzko, On the distribution of spacings between zeros of the zeta function, *Math. Comput.* **48**, 273 (1987); The 10^{22} -nd zero of the Riemann zeta function, in *Dynamical, Spectral, and Arithmetic Zeta Functions*, edited by M. van Frankenhuysen and M. L. Lapidus, American Mathematics Society, Contemporary Mathematics Series (AMS, Providence, 2001).
- [40] W.-J. Rao, Higher-order level spacings in random matrix theory based on Wigner’s conjecture, *Phys. Rev. B* **102**, 054202 (2020).
- [41] A. Y. Abul-Magd and M. H. Simbel, Wigner surmise for high-order level spacing distributions of chaotic systems, *Phys. Rev. E* **60**, 5371 (1999).
- [42] J. von Neumann and E. P. Wigner, Über das Verhalten von Eigenwerten bei adiabatischen Prozessen, in *The Collected Works of Eugene Paul Wigner*, edited by A. S. Wightman (Part A: The Scientific Papers. Part B: Historical, Philosophical, and Socio-Political Papers), Vol. A/1 (Springer, Berlin, Heidelberg, 1993), pp. 294–297.
- [43] J. B. Keller, Multiple eigenvalues, *Lin. Alg. Appl.* **429**, 2209 (2008).
- [44] A. L. Andrew, Eigenvectors of certain matrices, *Lin. Alg. Appl.* **7**, 151 (1973).
- [45] A. Cantori and F. Butler, Eigenvalues and eigenvectors of symmetric centrosymmetric matrices, *Lin. Alg. Appl.* **13**, 275 (1976).
- [46] C. Hammond and S. J. Miller, Eigenvalue spacing distribution for the ensemble of real symmetric Toeplitz matrices, *J. Theor. Prob.* **18**, 537 (2005).
- [47] W. Bryc, A. Dembo, and T. Jiang, Spectral measure of large random Hankel, Markov and Toeplitz matrices, *Ann. Probab.* **34**, 1 (2006).
- [48] F. Haake, in *Quantum Signatures of Chaos, Quantum Coherence in Mesoscopic Systems*, edited by B. Kramer, NATO ASI Series Vol 254 (Springer, Boston, 1991).
- [49] F. Evers and A. D. Mirlin, Anderson transitions, *Rev. Mod. Phys.* **80**, 1355 (2008).
- [50] A. D. Mirlin, Y. V. Fyodorov, A. Mildnerberger, and F. Evers, Exact Relations between Multifractal Exponents at the Anderson Transition, *Phys. Rev. Lett.* **97**, 046803 (2006).
- [51] E. Bogomolny and O. Giraud, Eigenfunction Entropy and Spectral Compressibility for Critical Random Matrix Ensembles, *Phys. Rev. Lett.* **106**, 044101 (2011).
- [52] Y. Y. Atas, E. Bogomolny, O. Giraud, P. Vivo, and E. Vivo, Joint probability densities of level spacing ratios in random matrices, *J. Phys. A: Math. Theor.* **46**, 355204 (2013).